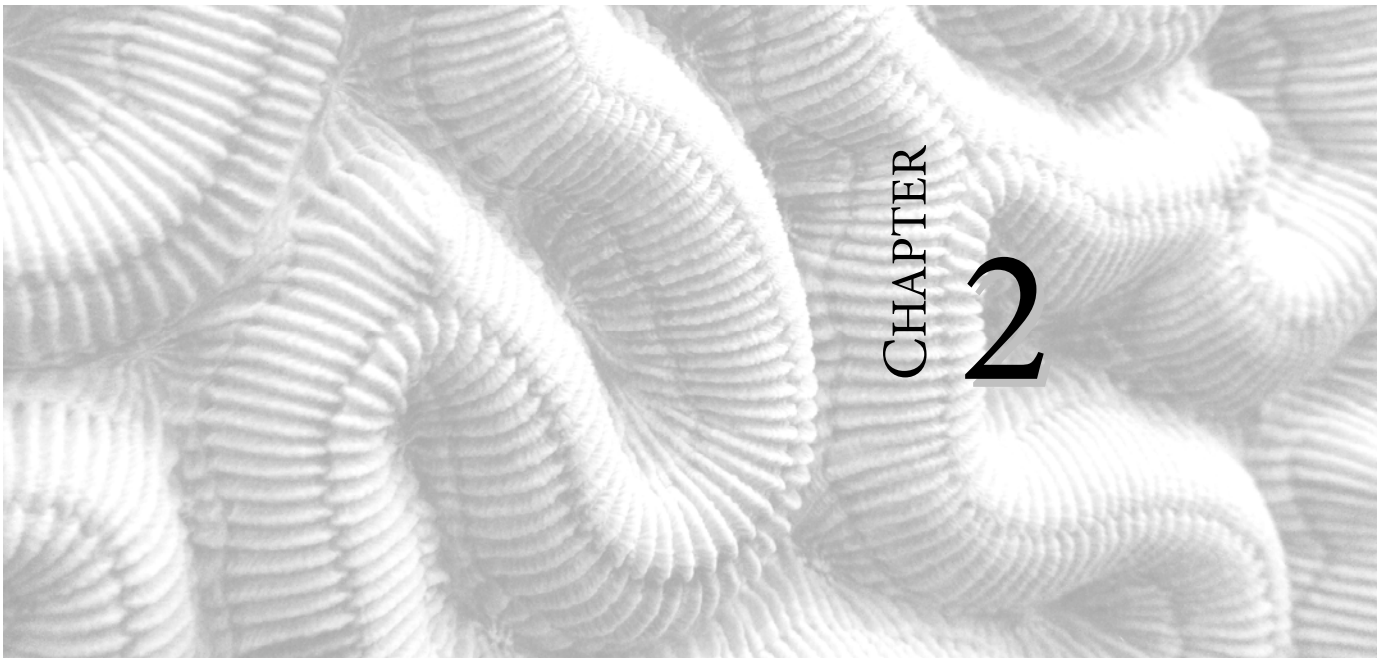

CHAPTER 2

HISTOPATHOLOGIC CORRELATE OF A SPECIFIC MRI FEATURE IN WHITE MATTER DISORDERS

CHAPTER 2.1

HISTOPATHOLOGIC CORRELATES OF RADIAL STRIPES ON MR IMAGES IN LYSOSOMAL STORAGE DISORDERS

J. Patrick van der Voorn
Petra J.W. Pouwels
Wout Kamphorst
James M. Powers,
Martin Lammens
Frederik Barkhof
Marjo S. van der Knaap

Am J Neuroradiol. 2005 Mar;26(3):442-6

Abstract

Background and purpose:
Radially oriented hypointense stripes in hyperintense cerebral white matter are recognized on T2-weighted images of certain lysosomal storage disorders. We compared in vivo and postmortem MR imaging findings with histopathologic findings in three patients with metachromatic leukodystrophy (MLD), globoid cell leukodystrophy (GLD) and infantile GM1 gangliosidosis (GM1) to understand this characteristic MR imaging pattern.
Methods:
The in vivo MR imaging protocol comprised T1- and T2- weighted spin echo, and FLAIR images. A postmortem MR imaging study of coronal 1-cm thick brain slices was performed after at least 5 weeks of Formalin fixation, and included T2-weighted spin echo images, and three-dimensional (3D)-FLAIR images with high spatial resolution. Afterwards the slices were embedded in paraffin, whole-mount sections were made and neuropathologic stains were applied.
Results:
Similar imaging features were found in the three examined patients on in vivo and postmortem imaging, with more prominent stripes in GLD and MLD than in GM1. Neuropathologic examination revealed that the stripes were related to relative sparing of myelin in the perivenular regions in GM1 and MLD, but lipid-containing glial cells were also present in these areas in MLD. Perivenular clusters of globoid cells containing lipid material in absence of any myelin corresponded to the stripes in GLD.
Conclusion:
Results of our postmortem study shows that radial stripes of white matter on MR images represented relative myelin sparing in some lysosomal storage disorders, but they may also represent lipid storage.

Introduction

MR imaging is highly sensitive in the detection of white matter lesions. Based on the distinct pattern of distribution of these lesions it is possible to discriminate between a large number of different white matter disorders [1]. Unfortunately, MR imaging has a limited specificity with regard to the underlying pathology of white matter abnormalities [2].

Previous reports of MR imaging studies in patients with MLD and GLD have described symmetric diffuse high signal on T2-weighted images throughout the cerebral white matter with radially oriented stripes of low signal intensity [3-6]. This same characteristic MR imaging pattern can also be seen in patients with GM1 (personal observations, [J.P.v.d.V., M.S.v.d.K.]). The pattern in these lysosomal storage disorders is thought to represent a lack of myelin with perivenular sparing of myelin [3-6]. However, this hypothesis does not find support in published case reports on the histopathology of the respective disorders [7-9].

To understand the observed MR imaging findings in the three lysosomal storage disorders we conducted postmortem MR imaging and histopathologic correlative studies of brains from patients who were diagnosed with MLD, GLD and infantile GM1, and had *in vivo* MR imaging before death.

Methods

Three patients with the three different lysosomal storage disorders, infantile GM1, MLD and GLD (see table 1 for details) were included in our study. All examinations were performed on a 1.5 T MR scanner (Siemens Vision, Erlangen, Germany). The standard in vivo imaging protocol for the brain included in all patients sagittal and transverse T1- (repetition time (TR) 570 ms, echo time (TE) 14 ms, excitations, 2) and T2- (TR 3000 ms, TE 22, 60 and 120 ms, excitations, 1) weighted spin echo images, and coronal or transverse FLAIR images (TR 9000 ms, TE 105 ms, inversion time (TI) 2200 ms, excitations, 1).

The parents signed informed consent for both postmortem MR imaging and brain autopsy. The patients came to autopsy within 6 hours after death, limiting the impact of autolysis. Postmortem imaging of the brain was performed after at least 5 weeks of Formalin fixation. The brains were cut into 1-cm thick coronal slices and for each patient four or five slices were selected that were subjected to MR imaging. The fixed 1-cm thick brain slices were put on plastic layers, 2 cm apart, into the "brain slice holder", a specially fabricated device for simultaneous MR imaging of up to seven brain slices in one session, which fits in the MR head coil [as described in 10].

The standard postmortem imaging protocol for the fixed brain slices included T2-weighted spin echo images, and multi-slab 3D-FLAIR images. Imaging parameters of the postmortem T2-weighted spin-echo sequence were: TR 2000 ms, TE 20 and 45 ms; excitations, 1; matrix, 160 x 256; field of view, 125 x 200 mm; and total acquisition time, 5 min. The slice thickness was 5 mm and the in-plane resolution was 1 mm2. The imaging slices were located at the center of the brain slices. In addition, a multi-slab 3D-FLAIR

sequence was used with high spatial resolution, consisting of six 1-cm thick slabs with 8 partitions each, resulting in a slice thickness of 1.25 mm with the following parameters: TR, 6500 ms; TE, 120 ms; TI, 2200 ms; matrix, 162 x 256; field of view, 127 x 200 mm and in-plane resolution of 0.78 x 0.78 mm; total acquisition time, 8 min. It is based on a turbo spin-echo imaging sequence, using a turbofactor of 27 [11,12]. The multi-slab nature of this sequence was used to fit the design of the box, selecting both the slab thickness and the gap between the slabs to be 1 cm.

After imaging, the coronal brain-slices were cut in half using a 5-mm deep cutting device, ensuring that the cut surface of the halved slice corresponded with the imaging plane of the T2-sequence [10].

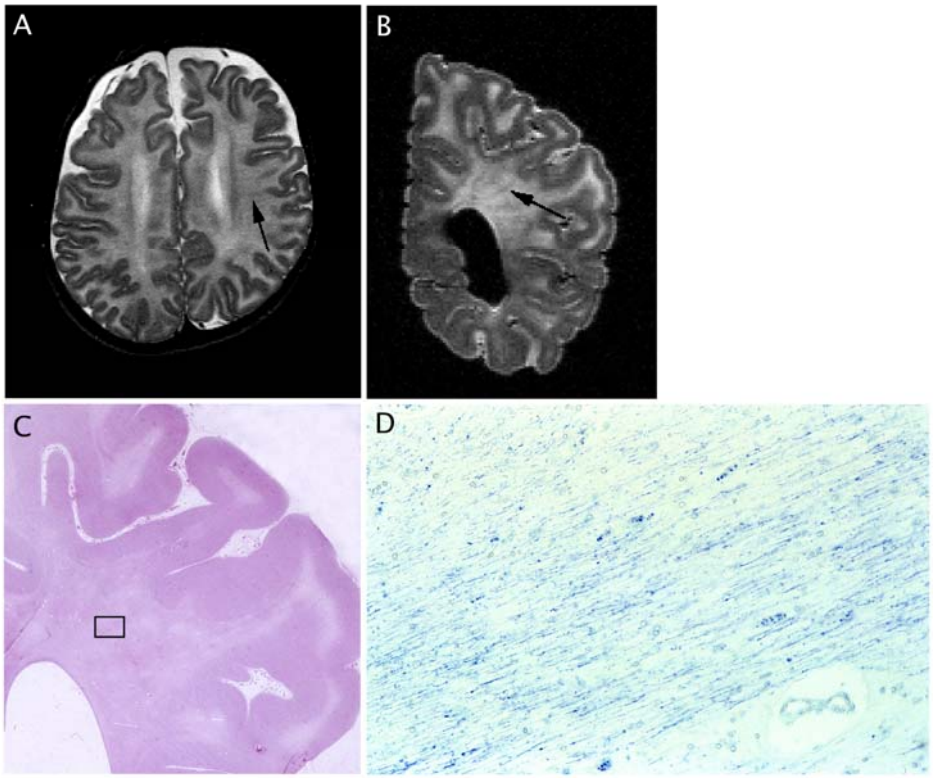

Figure 1. Patient 1, who had GM-1.
A and B, In vivo transverse T2-weighted image (A) and postmortem coronal 3D-FLAIR image (B) show a diffuse and symmetric increase in signal intensity in the cerebral white matter with radial stripes of low signal intensity (arrows).
C and D, Photomicrograph (hematoxylin and eosin; original magnification, x1.5) of matched histopathologic section (C) and magnified view (Luxol fast blue; original magnification, x75) of the small box in C (D) reveal perivenular areas of relatively normal density of myelin sheaths (blue in D, v: venules), within the hypomyelinated central white matter (top left and bottom right in D), corresponding to the hypointense stripes on MR imaging.

Subsequently, the slices were embedded in paraffin, and whole-mount 7-µm-thick sections were made. Routine neuropathologic staining techniques were applied to these paraffin sections, including hematoxylin and eosin (H&E), Luxol fast blue (LFB) to delineate areas of myelin breakdown and Bodian silver impregnations to determine axonal density. Immunohistochemical staining was performed on selected (smaller) 5-µm-thick paraffin-embedded sections, using the streptavidin-biotin complex procedure. The following primary antibodies were used: macrophage-specific marker KP1 (CD68) and leukocyte common antigen (CD45) for the presence of inflammatory cells and glial fibrillary acidic protein (GFAP) to evaluate the intensity of astrogliosis. The H&E sections were used to verify whether the histological sections matched the contours of the corresponding MR images. The areas corresponding to hypointense stripes on the 3D-FLAIR post mortem MR images were specifically compared with the matched areas on the histological sections.

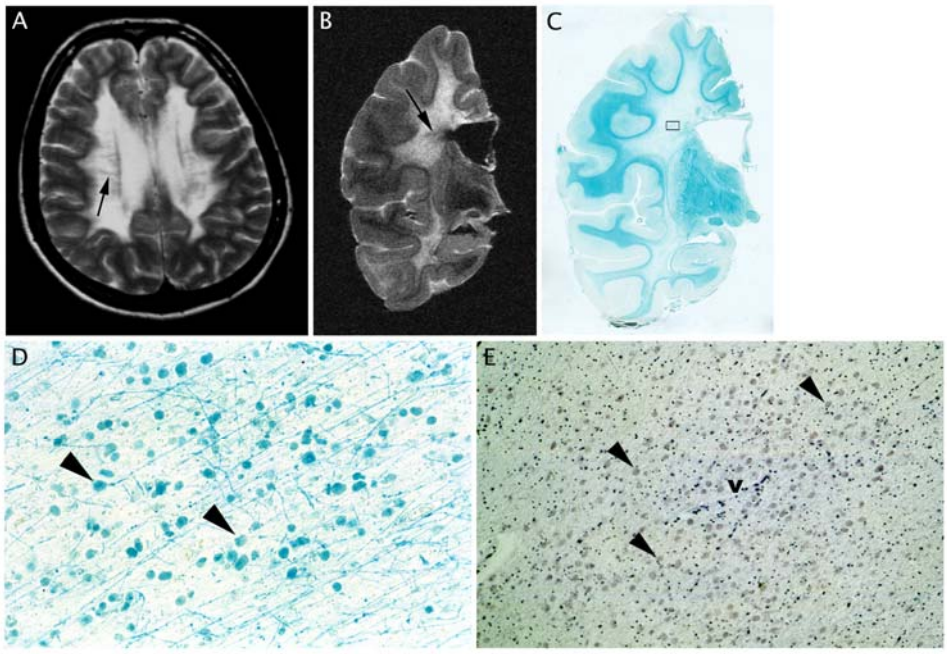

Figure 2. Patient 2, who had MLD.
A and B, In vivo transverse T2-weighted image (A) and postmortem coronal 3D-FLAIR image (B) show a hyperintense centrum semiovale with radially oriented stripes of hypointense signal (arrows).
C, Photomicrograph (Luxol fast blue; original magnification, x1) (C) demonstrates a profound absence of myelin throughout the centrum semiovale with some sparing of the subcortical U-fiber areas.
D and E, Magnified views of hematoxylin and eosin, (D; original magnification, x37,5) and Luxol fast blue, (E; original magnification, x75), of the small box in C show that the hypointense linear bands correspond with numerous eosinophilic granule containing glial cells and macrophages (arrowheads) around venules (v) and myelin (blue stripes in E).

Table 1: Summary of clinical characteristics of patients

Patient (no.) / Sex	Disorder	Age at MRI (y,m)	Neurological details
1 / M	Infantile GM1	0y7m	Presented at age 5 months with a failure to thrive. Progressively deteriorated with hypotonia, poor head control and poor visual contact and died at age 13 months.
2 / F	MLD	17y0m	Symptoms started at age 16 years with walking and learning problems. Died 1 month after bone marrow transplantation at age 18 years and 3 months.
3 / F	GLD	0y6m 0y11m	Feeding difficulties and poor visual response at age 3 months, developed hypertonia, increased irritability and epilepsy. Deteriorated rapidly and died at 1 year of age.

Note.—GM1 indicates infantile GM1 Gangliosidosis; MLD, Metachromatic Leukodystrophy; GLD, Globoid cell Leukodystrophy

RESULTS

Figures 1, 2 and 3 show in vivo, postmortem and histopathologic findings of the patients with GM1, MLD and GLD, respectively.

In vivo T2-weighted images demonstrated a diffuse and symmetrical increase in signal intensity throughout the cerebral white matter in all three patients. Within the affected white matter dots and stripes with low signal intensity were seen (comparable to findings in myelinated white matter), with a punctate pattern on the superior and a radial pattern on the inferior transverse T2-weighted images. Coronal FLAIR images displayed a pattern of radial stripes of low signal intensity within the hyperintense white matter, the stripes extending from the cerebral cortex to the ventricular wall. On the T1-weighted images the stripes had a normal high signal, whereas the remainder of the cerebral white matter had an abnormally low signal intensity. The stripes were more prominent in the GLD and MLD patients than in the GM-1 patient.

The T2-weighted and 3D-FLAIR images obtained in the Formalin-fixed coronal brain slices of the three patients revealed similar MR findings: a hyperintense centrum semiovale with radially oriented stripes of relatively normal, hypointense signal. Neuropathologic evaluation of the white matter in GM-1 demonstrated a diffuse paucity of myelin on LFB-stained sections and a commensurate loss of oligodendrocytes with relative sparing of axons on Bodian silver impregnations. Mild astrogliosis was observed in the white matter, with a few CD-68 positive macrophages. Microscopic study of the matched LFB-stained sections showed that the hypointense stripes on MR imaging represented perivenular areas of relatively increased myelin within the otherwise hypomyelinated central white matter. In these areas oligodendrocytes were better preserved (Figure 1).

The major neuropathologic changes in the MLD brain consisted of extensive demyelination throughout the white matter with some sparing of the subcortical U-fibers and with numerous reactive astrocytes and macrophages with eosinophilic granules. Exact correlation of the 3D-FLAIR images with LFB-stained sections showed that the hypointense bands corresponded with perivenular areas of myelin. Lipid containing glial cells and macrophages were also clustered in these areas of myelin (Figure 2).
Neuropathologic examination of the atrophic GLD brain was characterized by diffuse to nearly complete loss of myelin and dense astrogliosis. In these areas marked axonal loss was seen and oligodendrocytes were diminished. Multinucleated globoid cells (cells of phagocytic lineage containing large amounts of lipids) were clustered around blood vessels. The areas of hyperintensity on T2-weighted MRI corresponded to myelin-deficient foci and the hypointense stripes corresponded to the perivascular clustering of globoid cells, and not to (relatively preserved) myelin (Figure 3).

Discussion

We describe a peculiar MR imaging appearance, consisting of radially oriented stripes of apparently normal signal intensity within the otherwise diffusely abnormal cerebral white matter, in three patients with lysosomal diseases. These stripes are characteristic of these lysosomal storage disorders; they are not seen in other diffuse leukoencephalopathies. They differ from the radiating stripes within the abnormal white matter typically seen in vanishing white matter (VWM) [13, 14]. In VWM the cerebral white matter becomes rarefied and cystic and within the rarefied and cystic white matter, which has a low signal on proton density and FLAIR images, radiating stripes of remaining tissues strands are seen, but the stripes have an abnormally high signal. The stripes in VWM are not visible on T2-weighted images, because both the rarefied and cystic white matter and the strands of abnormal tissues have a high signal intensity [13, 14].

The stripes in lysosomal storage disorders were thought to represent perivenular sparing of myelin [3-6], but their nature has not been investigated before. We performed postmortem MR imaging with histopathologic correlation to understand the neuropathologic basis underlying this MR imaging pattern. Similar imaging features were found in the three examined patients on *in vivo* and postmortem imaging. The MRI visible stripes were rather subtle in GM-1. Histopathologic studies confirmed that the stripes were related to relative presence of myelin in this disease. The MRI visible stripes were more prominent in GLD and MLD and histopathologic studies showed that the situation was more complex in these disorders. In MLD we found that in the perivenular regions, corresponding to the stripes on MRI, myelin was relatively more prominent but that in these areas there was also an accumulation of glial cells and macrophages containing lipids. In GLD many globoid cells containing lipid material in the perivenular regions in absence of any myelin corresponded to the stripes on MRI. The high cell density and, most of all, the high content of stored lipids in these cells, most likely contribute to shortening of both T2 and T1 values.

Postmortem MR imaging of Formalin-fixed brain specimens can be easily performed on a standard MR scanner. The multi-slab 3D-FLAIR sequence, recently reported for the detection of lesions in patients with multiple sclerosis [11,12], provides thin slices with a high signal-to-noise ratio and allows direct histopathologic correlation with signal abnormalities on MR.

The findings at postmortem MR imaging, performed after Formalin fixation, qualitatively correlate well with the *in vivo* imaging findings. Formalin interposes itself between side groups of certain amino acids, thereby causing cross-linking and restricting mobility of molecules in the tissue after fixation. After tissue-fixation in Formalin, T1 and T2 relaxation times are reduced with the most rapid changes during the first 1 to 2 weeks, reaching a plateau by the 5th week [15-18]. For this reason, we used slightly adapted echo-times (shorter relative to in vivo studies) in the T2-weighted imaging for the study of the Formalin-fixed tissue. Despite the shortening of T1 and T2 relaxation time secondary to Formalin fixation, the gray-white matter differentiation and heterogeneity of signal intensity within the white matter remain evident on postmortem T2-weighted imaging.

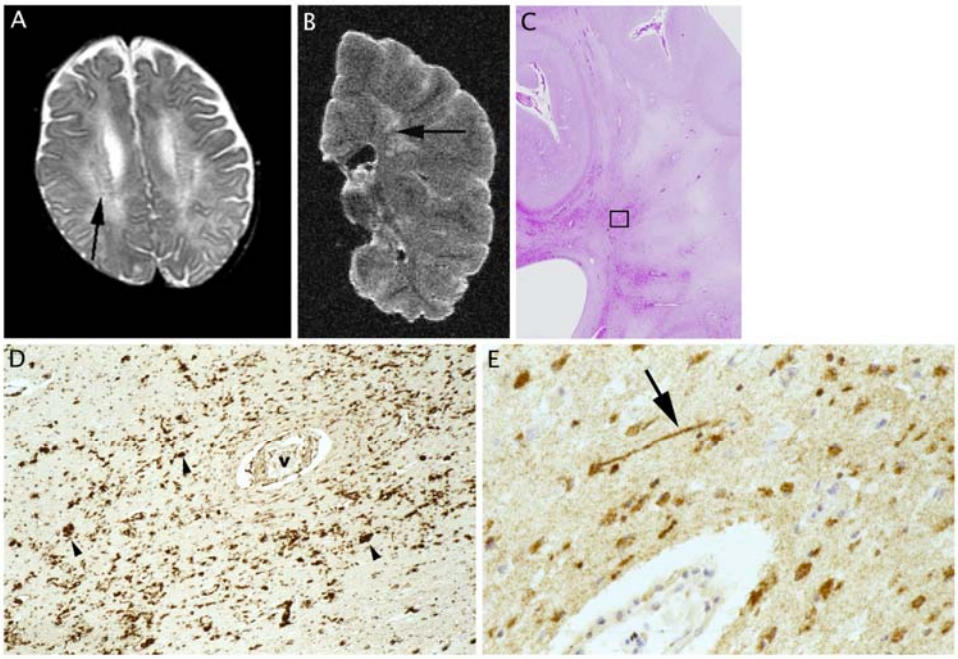

Figure 3. Patient 3, who had GLD.
A and B, In vivo transverse T2-weighted image (A) and postmortem coronal 3D-FLAIR image (B) show an atrophic brain with hyperintense white matter and linear areas of hypointense signal, extending from the cerebral cortex to the ventricular wall (arrows).
C and D, Photomicrograph of hematoxylin and eosin staining (C, original magnification, x1,5) and magnified view of CD68 staining (D, original magnification, x37,5) of the small box in C show perivascular clustering of multinucleated globoid cells (arrowheads, v: venule).
E, MBP-staining (original magnification, x75).shows almost complete absence of myelin sheaths (arrow).

The multi-slab 3D-FLAIR sequence was used in the postmortem MR imaging protocol to obtain thin sections, which allowed good matching with the whole-mount histopathologic sections. However, 3D-FLAIR imaging is not essential to demonstrate the stripes *in vivo* in patients with these lysosomal white matter disorders. Conventional T2-weighted imaging on a standard scanner will reveal the stripes in the diffusely affected white matter, which may be helpful in distinguishing these disorders from other leukoencephalopathies.

Conclusion

Our results show that different histopathologic correlates are responsible for a similar characteristic MR imaging pattern in three lysosomal storage disorders. Postmortem imaging followed by correlative histopathology can help to elucidate the histopathologic basis of imaging features in white matter disorders.

Acknowledgments

We thank Hugo Vrenken for his assistance in the postmortem MR imaging measurements. We are also grateful to Jaap van Veldhuisen and Ron Otsen for their artistic graphic support.

REFERENCES

1. Van der Knaap MS, Breiter SN, Naidu S et al. Defining and categorizing leukoencephalopathies of unknown origin: MR imaging approach. Radiology 1999; 213:121-133

2. Van der Knaap MS Magnetic resonance in childhood white-matter disorders. Dev Med Child Neurol 2001; 43: 705-712

3. Faerber EN, Melvin JJ, Smergel EM. MRI appearances of metachromatic leukodystrophy. Pediatr Radiol 1999; 29:669-672

4. Kim IO, Kim WS. MR of childhood metachromatic leukodystrophy. AJNR Am J Neuroradiol 1997; 18:733-738

5. Sasaki M, Sakuragawa N, Takashima S, Hanaoka S. MRI and CT findings in Krabbe disease. Pediatr Neurol 1991; 7:283-8

6. Barkovich AJ. Concepts of myelin and myelination in neuroradiology. AJNR Am J Neuroradiol 2000; 21:1099-1109

7. Folkerth RD, Alroy J, Bhan I, Kaye EM. Infantile GM1 gangliosidosis: complete morphology and histochemistry of two autopsy cases with particular reference to delayed central nervous system myelination. Pediatr Dev Pathol 2000; 3:73-86

8. Haberland C, Brunngraber E, Witting L, Daniels A. Juvenile metachromatic leucodystrophy. Case report with clinical, histopathological, ultrastructural and biochemical observations. Acta Neuropathol 1973; 26:93-106

9. Percy AK, Odrezin GT, Knowles PD, Rouah E, Armstrong DD. Globoid cell leukodystrophy: comparison of neuropathology with magnetic resonance imaging. Acta Neuropathol 1994; 88:26-32

10. Bö L. Geurts JJG, Ravid R, Barkhof F. Magnetic resonance imaging as a tool to examine the neuropathology of multiple sclerosis. Neuropathol Appl Neurobiol 2004; 2:106-17

11. Tan IL, Pouwels PJ, van Schijndel RA, Ader HJ, Manoliu RA, Barkhof F. Isotropic 3D fast FLAIR imaging of the brain in multiple sclerosis patients: initial experience. Eur Radiol 2002; 12:559-67 12.

12. Tan IL, van Schijndel RA, Pouwels PJ, Ader HJ, Barkhof F. Serial isotropic three-dimensional fast FLAIR imaging: using image registration and subtraction to reveal active multiple sclerosis lesions. AJR Am J Roentgenol 2002; 179:777-82

13. Van der Knaap MS, Barth PG, Gabreëls FJM, Franzoni E, Begeer JH, Stroink H, Rotteveel JJ, Valk J. A new leukoencephalopathy with vanishing white matter. Neurology 1997; 48: 845-855.

14. Van der Knaap MS, Kamphorst W, Barth PG, Kraaijeveld CL, Gut E, Valk J. Phenotypic variation in leukoencephalopathy with vanishing white matter. Neurology 1998; 51: 540-547

15. Tovi M and Ericsson A. Measurements of T1 and T2 over time in formalin-fixed human whole-brain specimens. Acta Radiol 1992; 33:400-4

16. Blamire AM, Rowe JG, Styles P, McDonald B. Optimising imaging parameters for post mortem MR imaging of the human brain. Acta Radiol 1999; 40:593-597

17. Thickman DI, Kundel HL, Wolf G. Nuclear magnetic resonance characteristics of fresh and fixed tissue: the effect of elapsed time. Radiology 1983; 148:183-185

18. Van den Hauwe L, Parizel PM, Martin JJ, Cras P, De Deyn P, De Schepper AMA. Postmortem MRI of the brain with neuropathological correlation. Neuroradiology 1995; 37:343-349.

.